

# Novel nonlinear stiffness parameters and constitutive curves for concrete

Rajai Z. Al-Rousan\*, Mohammed A. Alhassan and Moheldeen A. Hejazi

Department of Civil Engineering, Jordan University of Science and Technology, Irbid, Jordan

(Received August 4, 2018, Revised December 15, 2018, Accepted December 17, 2018)

**Abstract.** Concrete is highly non-linear material which is originating from the transition zone in the form of micro-cracks, governs material response under various loadings. In this paper, the constitutive models published by many researchers have been used to generate novel stiffness parameters and constitutive curves for concrete. Following such linear material formulations, where the energy is conservative during the curvature, and a nonlinear contribution to the concrete has been made and investigated. In which, nonlinear concrete elastic modulus modeling has been developed that is capable-of representing concrete elasticity for grades ranging from 10 to 140 MPa. Thus, covering the grades range of concrete up to the ultra-high strength concrete, and replacing many concrete models that are valid for narrow ranges of concrete strength grades. This has been followed by the introduction of the nonlinear Hooke's law for the concrete material through the replacement of the Young constant modulus with the nonlinear modulus. In addition, the concept of concrete elasticity index ( $\phi$ ) has been proposed and this factor has been introduced to account for the degradation of concrete stiffness in compression under increased loading as well as the multi-stages micro-cracking behavior of concrete under uniaxial compression. Finally, a sub-routine artificial neural network model has been developed to capture the concrete behavior that has been introduced to facilitate the prediction of concrete properties under increased loading.

**Keywords:** nonlinear elasticity index; constitutive relations; Nonlinear Hooke's Law; nonlinear strain energy density; concrete; artificial neural network

## 1. Introduction

In structural analysis, the accurate estimation of elastic modulus is essential, and it determines in the first place, the reliability of the analysis and predicted results. Therefore, many studies have been carried out to establish approximate models that can capture structural materials constitutive behavior and elastic modulus of different materials (Akhilesh 2013, Jiong *et al.* 2015, Maiga *et al.* 2015, Lino and Farhad 2016, Mehrzad *et al.* 2017, Sharif *et al.* 2017, Jiong *et al.* 2017). For structural steel, there is a well-defined elastic region in the stress-strain curve. However, for concrete analysis, there is no single value nor the single definition of elastic modulus to be used in the analysis since concrete behaves in a non-linear manner. To account for the non-linear behavior, design codes have proposed many equations for the estimation of the elastic modulus using the secant modulus definition; represented by the slope of a line drawn from initial loading up to a stress of 0.4 to 0.5 of concrete strength. This definition, however, provides a constant value for concrete elastic modulus  $E_c$ , ignoring the stress-dependent nature of concrete elastic modulus. Which can be described with higher accuracy if the tangent modulus; (the instantaneous slope of stress-strain curve), is to be incorporated in concrete elastic modulus estimation.

Different design codes offer various equations for the estimation of elastic modulus. These equations capture the

dependency of  $E_c$  on concrete strength and density, for normal-weight and light-weight concrete up to 120 MPa.

### 1.1 ACI 318-14 code

In 1960, based on earlier studies. Pauw (1960) proposed the use of the square root of concrete compressive strength in the estimation of  $E_c$ , accounting for concrete density for normal and lightweight concrete. Pauw's proposed formula has the form

$$E_c = a \cdot w_c^{3/2} \cdot \sqrt{f'_c} \quad (1)$$

Since 1963, ACI 318 (1963) has adopted the use of Pauw formula in Elastic modulus estimation. the secant definition is used by ACI 318-14 (2014) as the slope of the stress-strain curve from zero stress up to 0.45 concrete strength ( $f'_c$ ) with a discrepancy in the measured  $E_c$  value of  $\pm 20\%$ . Recent ACI 318-14 (2014) (Sec. 19.2.2.1) permits the use of the following two equations for the estimation of the concrete elastic modulus ( $E_c$ ).

$$E_c = w_c^{1.5} \cdot 0.043 \cdot \sqrt{f'_c} \quad (2)$$

$$E_c = 4700 \cdot \sqrt{f'_c} \quad (3)$$

These two equations yield good accuracy for concrete grades up to 42 MPa. However, for higher grades, these equations tend to overestimate concrete modulus of elasticity. This led to another equation being suggested by ACI committee-363 for high strength concrete (ACI363 1997, Nilson *et al.* 2010).

\*Corresponding author, Ph.D.  
E-mail: rzalrousan@just.edu.jo

### 1.2 ACI 363R-92

ACI committee 363 (1997) has proposed the use of the following expression for the estimation of the elastic modulus of concrete grades higher than 41 MPa. This equation is based on studies done by Carraquillo *et al.* (1981), Martinez *et al.* in (1984) on high strength concrete, yielding improved results for concrete grades between 20 MPa and 82 MPa (ACI363 1997, Nilson *et al.* 2010, Carraquillo *et al.* 1981, Martinez *et al.* in 1984)). The proposed equation is given as

$$E_c = (3320 \cdot \sqrt{f'_c} + 6900) \times \left(\frac{w_c}{2300}\right)^{1.5} \quad (4)$$

### 1.3 Eurocode-2

Eurocode-2 (2004) adopts the use of the cube root of the concrete compressive strength  $f'_c$  in elastic modulus estimation. The slope of the stress-strain curve from zero stress to  $0.4 f'_c$ , being the definition of secant modulus as per Eurocode-2 (2004). The following equation is permitted to be used in elastic modulus estimation

$$E_c = 22,000 \left(\frac{f'_c}{10}\right)^{1/3} \quad (5)$$

### 1.4 CEB - FIB MC2010

MC2010 (2010) issued by the International Federation for Structural Concrete uses a similar definition for the elastic modulus as per Eurocode-2 (2004); that's, the secant modulus is taken up to  $0.4 f'_c$ . MC2010 (2010) however, defines concrete elastic modulus as a reduced value of the initial tangent modulus, which is assumed to be the unloading elastic modulus. The reduction of the initial modulus is to account for initial plastic strains. In MC2010 (2010), the elastic modulus is given by

$$E_c = 21.5 \times 10^3 \cdot \alpha_i \cdot \alpha_E \cdot \left(\frac{f'_c}{10}\right)^{1/3} \quad (6)$$

where:  $\alpha_E$  is a factor accounting for aggregate type, it's equal to 1 and 0.9 for quartzite and limestone aggregate, respectively.  $\alpha_i$  is a factor accounting for initial plastic deformation, and it is given by the expression

$$\alpha_i = 0.8 + 0.2 \cdot \frac{f'_c}{88} \leq 1 \quad (7)$$

### 1.5 Noguchi, Tomosawa, Nemati, *et al.*

In 2009, Noguchi *et al.* have collected data for more than 3000 concrete samples made using various aggregate materials and admixtures. Having strength grades ranging from 40 MPa to 160 MPa. Through these data and statistical analysis and regression they introduced a simple equation that accounts for concrete grade, density, aggregates and admixtures. in their investigation, they concluded that the use of the cube root of concrete compressive strength and the density squared, yields better proportionality rather than the square root of the compressive strength and the density to the power 1.5, as per ACI 318 (2014), ACI 363 (1997)

Table 1 Values of aggregate and admixture correction factors (Noguchi *et al.* 2009)

Type of aggregate	$k_1$
Crushed limestone, calcined bauxite	1.20
Crushed (quartzitic, andesite, basalt, clay-slate, cobblestone) aggregate	0.95
Other than above	1.00
Type of additive	$k_2$
Silica fume, ground-granulated blast-furnace slag, fly ash fume	0.95
Fly ash	1.10
Other than above	1.00

and Noguchi *et al.* (2009). Noguchi *et al.* equation is as follows

$$E_c = k_1 k_2 \cdot 1.486 \times 10^{-3} \cdot f'_c \left(\frac{1}{3}\right) \cdot w_c^2 \quad (8)$$

where  $k_1$  and  $k_2$  are correction factors for coarse aggregate and admixtures respectively. The values for these factors are given in the Table 1. However, for ordinary mixtures,  $k_1$  and  $k_2$  are considered equal to 1.

### 1.6 Concrete relations hitherto

In the literature, there are many constitutive models that have been proposed to capture the stress-strain behaviour of concrete under uniaxial compression. Here to be considered, the most widely used models that are applicable to different ranges of concrete grades. The consideration of such variety is intended to produce general factors and conclusions, which apply to a wide range of concrete grades ranging from 16 to 120 MPa.

In 1951, Hognestad introduced one of the first constitutive models for concrete under uniaxial compression. In His model, the concrete stress-strain curve has been represented by two branches. The first being an ascending branch that follows a second-degree parabola till reaching the peak strength represented by  $0.85 f'_c$ ; maximum reliable strength. The second branch is a linear descending branch. Leading to the following equations

$$\frac{\sigma}{f'_c} = 2 \cdot \frac{\varepsilon}{\varepsilon_0} \cdot \left(1 - \frac{\varepsilon}{2\varepsilon_0}\right) \quad \text{For } 0 \leq \varepsilon \leq \varepsilon_0 \quad (9)$$

$$\frac{\sigma}{f'_c} = 1 - 0.15 \cdot \left(\frac{\varepsilon - \varepsilon_0}{\varepsilon_u - \varepsilon_0}\right) \quad \text{For } \varepsilon_0 \leq \varepsilon \leq \varepsilon_u \quad (10)$$

In this paper, however, the 0.85 factor in Hognestad model (1951) has been omitted in-order-to represent the complete ascending curve. In 1960, Rusch (1960) suggested the use of horizontal post-peak branch instead of the descending branch in Hognestad model, with  $\varepsilon_0=0.002$  and  $\varepsilon_u=0.0035$  for all concrete grades.

$$\frac{\sigma}{f'_c} = \left(2 \cdot \frac{\varepsilon}{\varepsilon_0} - \left(\frac{\varepsilon}{\varepsilon_0}\right)^2\right) \quad \text{For } 0 \leq \varepsilon \leq \varepsilon_0 \quad (11)$$

$$\frac{\sigma}{f'_c} = 1 \quad \text{For } \varepsilon_0 \leq \varepsilon \leq \varepsilon_u \quad (12)$$

In 1971, Kent and Park (1971) introduced a modification to Hognestad model (1951), by eliminating the strength reduction factor of 0.85, and by fixing the strain  $\varepsilon_0$  corresponding to  $f'_c$  at a value of 0.002 and defining the

Table 2 Equations of implemented concrete constitutive models

Label	Model	Equation	Range	Parameters	Domain of Consideration, MPa
H-51	Hognestad (1951)	$\frac{\sigma}{f'_c} = 2 \cdot \frac{\varepsilon}{\varepsilon_0} \cdot \left(1 - \frac{\varepsilon}{2 \cdot \varepsilon_0}\right)$ $\frac{\sigma}{f'_c} = 1 - 0.15 \cdot \left(\frac{\varepsilon - \varepsilon_0}{\varepsilon_u - \varepsilon_0}\right)$	$0 \leq \varepsilon \leq \varepsilon_0$ $\varepsilon_0 \leq \varepsilon \leq \varepsilon_u$	$\varepsilon_0 = 1.8 \cdot \frac{f'_c}{E_c}$	16 to 120
KP-71	Kent and Park (1971)	$\frac{\sigma}{f'_c} = 2 \cdot \frac{\varepsilon}{\varepsilon_0} \cdot \left(1 - \frac{\varepsilon}{2 \cdot \varepsilon_0}\right)$ $\frac{\sigma}{f'_c} = 1 - Z \cdot (\varepsilon - \varepsilon_0)$	$0 \leq \varepsilon \leq \varepsilon_0$ $\varepsilon_0 \leq \varepsilon \leq \varepsilon_u$	$\varepsilon_{50u} = \frac{3 + 0.29 \cdot f'_c}{145 \cdot f'_c - 1000}$ $Z = \frac{0.5}{\varepsilon_{50u} - \varepsilon_0}$ ; $\varepsilon_0 = 0.002$	16 to 40
P-73	Popovics (1970)	$\frac{\sigma}{f'_c} = \frac{n \cdot \left(\frac{\varepsilon}{\varepsilon_0}\right)}{(n-1) + \left(\frac{\varepsilon}{\varepsilon_0}\right)^n}$	$0 \leq \varepsilon \leq \varepsilon_u$	$n = 0.4 \times 10^{-3} \cdot f'_c + 1$ $\varepsilon_0 = 2.7 \times 10^{-4} \cdot \sqrt[4]{f'_c}$	16 to 70
T-87	Thorenfeldt <i>et al.</i> (1987)	$\frac{\sigma}{f'_c} = \frac{n \cdot \left(\frac{\varepsilon}{\varepsilon_0}\right)}{(n-1) + \left(\frac{\varepsilon}{\varepsilon_0}\right)^{kn}}$		$k=1$ , for $\varepsilon \leq \varepsilon_0$ $k = 0.67 + \frac{f'_c}{77.5}$ $\varepsilon \geq \varepsilon_0$ $n = \frac{E_{it}}{E_{it} - E_{cl}}$	16 to 40
R-60	Rüsch (1960)	$\frac{\sigma}{f'_c} = 2 \cdot \frac{\varepsilon}{\varepsilon_0} - \left(\frac{\varepsilon}{\varepsilon_0}\right)^2$ $\frac{\sigma}{f'_c} = 1$	$0 \leq \varepsilon \leq \varepsilon_0$ $\varepsilon_0 \leq \varepsilon \leq \varepsilon_u$	$\varepsilon_0 = 0.002$	16 to 40
GB-02	GB 50010 (2002)	$\frac{\sigma}{f'_c} = \left(1 - \left(1 - \frac{\varepsilon}{\varepsilon_0}\right)^n\right)$ $\frac{\sigma}{f'_c} = 1$	$0 \leq \varepsilon \leq \varepsilon_0$ $\varepsilon_0 \leq \varepsilon \leq \varepsilon_u$	$n = 2 - \frac{f_{cu} - 50}{60}$ $\varepsilon_0 = 0.002 + \frac{(f_{cu} - 50)}{2} \times 10^{-5}$ $\varepsilon_u = 0.0033 - (f_{cu} - 50) \times 10^{-5}$	16 to 40
CC-85	Carriera and Chu Model (1985)	$\frac{\sigma}{f'_c} = \frac{\beta \cdot \left(\frac{\varepsilon}{\varepsilon_0}\right)}{(\beta - 1) + \left(\frac{\varepsilon}{\varepsilon_0}\right)^\beta}$		$\beta = \frac{1}{1 - \left(\frac{f'_c}{\varepsilon_0 \cdot E_{it}}\right)}$ $E_{it} = \frac{f'_c}{\varepsilon_0} \cdot \left(\frac{24.82}{f'_c} + 0.92\right)$ $\varepsilon_0 = (1680 + 7.1 \cdot f'_c) \times 10^{-6}$	12 to 120
MC-10	CEB-FIB MC2010 (2010), Eurocode 2 (2004)	$\frac{\sigma}{f'_c} = \frac{k \cdot \eta - \eta^2}{1 + (k - 2) \cdot \eta}$	$0 \leq \varepsilon \leq \varepsilon_{c,lim}$	$k = E_{it}/E_{cl}$ ; $\eta = \varepsilon/\varepsilon_0$	12 to 120
LZ-10	Lu and Zhao (2010)	$\frac{\sigma}{f'_c} = \frac{(E_{it}/E_{cl}) \cdot (\varepsilon/\varepsilon_0) - (\varepsilon/\varepsilon_0)^2}{1 + ((E_{it}/E_{cl}) - 2) \cdot (\varepsilon/\varepsilon_0)}$	$0 \leq \varepsilon \leq \varepsilon_L$ $\varepsilon_L = \varepsilon_0 \left(\frac{1}{10} \frac{E_{it}}{E_{cl}} + \frac{4}{5} + \sqrt{\left(\frac{1}{10} \frac{E_{it}}{E_{cl}} + \frac{4}{5}\right)^2 - \frac{4}{5}}\right)$		12 to 120

descending branch with respect to a strain corresponding to  $0.5 f'_c$ .

$$\frac{\sigma}{f'_c} = 2 \cdot \frac{\varepsilon}{\varepsilon_0} \cdot \left(1 - \frac{\varepsilon}{2 \cdot \varepsilon_0}\right) \quad \text{For } 0 \leq \varepsilon \leq \varepsilon_0 \quad (13)$$

$$\frac{\sigma}{f'_c} = 1 - Z \cdot (\varepsilon - \varepsilon_0) \quad \text{For } \varepsilon_0 \leq \varepsilon \leq \varepsilon_u \quad (14)$$

where  $\varepsilon_0=0.002$  the strain corresponding to the peak stress,  $Z$  is the slope of the descending branch, given as  $Z=0.5/(\varepsilon_{50u}-\varepsilon_0)$ ,  $\varepsilon_{50u}=(3+0.29 f'_c)/(145 f'_c-1000)$  the strain in the descending branch corresponding to 0.5 the peak stress.

In 1973, Popovics (1970) represented both ascending and descending branches using the following equation

$$\frac{\sigma}{f'_c} = \frac{n \cdot \left(\frac{\varepsilon}{\varepsilon_0}\right)}{(n-1) + \left(\frac{\varepsilon}{\varepsilon_0}\right)^n} \quad (15)$$

where  $n=(0.4 \times 10^{-3} f'_c + 1)$ ,  $\varepsilon_0=2.7 \times 10^{-4} \times (f'_c)^{1/4}$  defined as strain at peak stress. In 1985, Based on Popovics model, Carriera and Chu (1985) introduced a modified model

capable of capturing the constitutive behaviour of high strength concrete up to 80 MPa. The general equation is identical to Popovics equation. However, in their model, they suggested more sophisticated means for estimating the factor  $\beta$ .

$$\frac{\sigma}{f'_c} = \frac{\beta \cdot \left(\frac{\varepsilon}{\varepsilon_0}\right)}{(\beta - 1) + \left(\frac{\varepsilon}{\varepsilon_0}\right)^\beta} \quad (16)$$

$$\beta = \frac{1}{1 - \left(\frac{f'_c}{\varepsilon_0 \cdot E_{it}}\right)} \quad (17)$$

$$E_{it} = \frac{f'_c}{\varepsilon_0} \cdot \left(\frac{24.82}{f'_c} + 0.92\right) \quad (18)$$

$$\varepsilon_0 = (1680 + 7.1 \cdot f'_c) \times 10^{-6} \quad (19)$$

where  $E_{it}$  is the initial tangent elastic modulus. Since 1993, International Federation for Structural Concrete FIB proposed a model based on work by Sargin and Handa (1969). MC Model can capture concrete constitutive

Table 3 Values of parameters required in the evaluation of different models

Label	Models	Concrete Grade, MPa															
		16	25	30	35	40	45	50	55	60	70	80	90	100	110	120	
H-51	Hognestad (1951)	$\varepsilon_0$ ( $10^{-3}$ )	1.4	1.9	2.1	2.3	2.5	2.7	2.9	3.0	3.2	3.5	3.7	4	4.3	4.5	4.7
		$\varepsilon_u$ ( $10^{-3}$ )									3.8						
KP-71	Kent and Park (1971)	$\varepsilon_0$ ( $10^{-3}$ )								2							
		$\varepsilon_u$ ( $10^{-3}$ )															
P-73	Popovics (1970)	$\varepsilon_0$ ( $10^{-3}$ )															
T-87	Thorenfeldt <i>et al.</i> (1987)	$\varepsilon_u$ ( $10^{-3}$ )								3.5							
R-60	Rüsch (1960)	$\varepsilon_0$ ( $10^{-3}$ )															
GB-02	GB 50010 (2002)	$\varepsilon_u$ ( $10^{-3}$ )					2				2.05	2.1	2.15	2.2	2.25	2.3	2.35
		$\varepsilon_c$ ( $10^{-3}$ )					3.3				3.25	3.2	3.1	3	2.9	2.8	2.7
CC-85	Carriera and Chu Model (1985)	$E_{it}$ , Gpa	22	25.7	27.7	29.6	31.4	33.1	34.8	36.4	38.0	41.0	43.8	46.4	48.9	51.2	53.4
		$\varepsilon_0$ ( $10^{-3}$ )	1.79	1.86	1.9			2			2.1	2.2	2.25	2.3	2.4	2.5	
MC-10	CEB-FIB MC2010 (2010), Eurocode 2 (2004)	$k$	2.36	2.15	2.04	1.92	1.82	1.74	1.66	1.61	1.55	1.47	1.41	1.36	1.32	1.24	1.18
		$\varepsilon_0$ ( $10^{-3}$ )	2	2.2	2.3	2.4	2.5	2.6	2.7	2.8	2.9	3					
LZ-10	Lu and Zhao (2010)	$\varepsilon_c, \text{lim}$ ( $10^{-3}$ )			3.5			3.4	3.4	3.3	3.2	3.1		3			
		$E_{it}/E_{cl}$	2.47	1.91	1.75	1.63	1.54	1.47	1.42	1.37	1.33	1.27	1.23	1.2	1.17	1.15	1.13
		$\varepsilon_0$ ( $10^{-3}$ )	2	2.2	2.3	2.4	2.5	2.6	2.7	2.8	2.9	3					
		$\varepsilon_c, \text{lim}$ ( $10^{-3}$ )	3.2	3.12	3.13	3.04	3.09	3.15	3.21	3.16	3.24	3.17	3.22	3.29	3.35	3.32	3.28

behaviour for a wide range of concrete grades, ranging from 12 MPa up to 120 MPa. In MC2010 (2010), the Model was given in two equations. However, the MC2010 (2010) equation describing the behaviour following the ultimate strain has been omitted, due to element size dependency.

$$\frac{\sigma}{f_c'} = \frac{k \cdot \eta - \eta^2}{1 + (k-2) \cdot \eta} \quad \text{For } \varepsilon \leq \varepsilon_{lim,c} \quad (20)$$

where  $k$  is plasticity number, ( $k=E_{it}/E_{cl}$ ).  $E_{it}$  is the initial tangent modulus and  $E_{cl}$  stands for the secant modulus sloping from zero to peak concrete stress.  $\eta$  denote the strain ratio ( $\eta=\varepsilon/\varepsilon_0$ ).

Based on Rusch model (1960), The Chinese National Standard GB50010 (2002) suggests some modified equations, yielding the same results for  $f_c' \leq 50$  MPa as Rusch model. These equations are as follows

$$\frac{\sigma}{f_c'} = \left(1 - \left(1 - \frac{\varepsilon}{\varepsilon_0}\right)^n\right) \quad \text{For } 0 \leq \varepsilon \leq \varepsilon_0 \quad (21)$$

$$\frac{\sigma}{f_c'} = 1 \quad \text{For } \varepsilon_0 \leq \varepsilon \leq \varepsilon_u \quad (22)$$

where  $n=(2-(f_{cu}-50)/60)$ ,  $\varepsilon_0=(0.002+0.5 \cdot (f_{cu}-50) \times 10^{-5})$ ,  $\varepsilon_u=(0.0033-(f_{cu}-50) \times 10^{-5})$ . In 2010, Lu and Zhao (2010) proposed a constitutive model by combining different models. It has been shown that Lu and Zhao Model (2010) gives the higher accuracy in predicting concrete constitutive behaviour for grades in the range 50-140 MPa.

$$\frac{\sigma}{f_c'} = \frac{(E_{it}/E_{cl}) \cdot (\varepsilon/\varepsilon_0) - (\varepsilon/\varepsilon_0)^2}{1 + (E_{it}/E_{cl} - 2) \cdot (\varepsilon/\varepsilon_0)} \quad (23)$$

$$\frac{\sigma}{f_c'} = \frac{1}{1 + 0.25 \cdot (\varepsilon/\varepsilon_0 - \varepsilon_0/\varepsilon_L - 1)^{1.5}} \quad (24)$$

This equation is the same as that proposed by fib MC2010 (2010). However, the difference appears in the

estimation of  $E_{it}$ ,  $E_{cl}$ ,  $\varepsilon_0$  and the strain value beyond which this equation is no more valid. Equations defining all preceding models have been summarized in Table 2. Equations of different factors and parameters are also provided for convenience.

## 2. Concrete nonlinear elasticity Index

### 2.1 Stress-Strain models analysis

In this investigation, the Constitutive models proposed by many researchers are to be used, to generate stress-strain curves. The consideration of many models is to account for various shapes of concrete stress-strain diagrams, which results due to the randomness of mixtures, compositions and material sources, used in the development of each model. Concrete stress-strain diagrams for concrete grades ranging from 16 to 120 MPa are to be considered. That's, C16, C25, C30, C35, C40, C45, C50, C55, C60, C70, C80, C90, C100, C110, C120. The designation of concrete grades is based on cylinder strength as per MC2010 (2010). Each model behavior has been investigated for the entire range of concrete grades to examine stability and results-reliability of different models in comparison to more refined ones. The parameters used in defining models for each concrete grade are summarized in Table 3.

The trend of different models with normalized stress values is shown in Fig. 1. The response of models (Fig. 1) in concern is converging from initial loading up to elasticity limit as established by various codes provisions. However, the scatter resulting from adopting  $0.4 f_c'$ , as per Eurocode 2 (2004) and Fib MC2010 (2010), is lower than that of 0.45

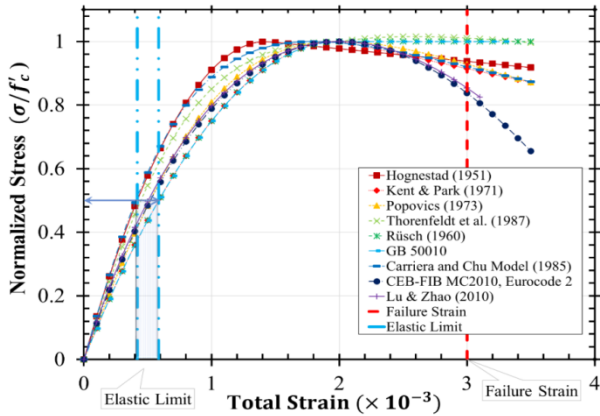


Fig. 1 Normalized Stress-Strain diagrams based on various models

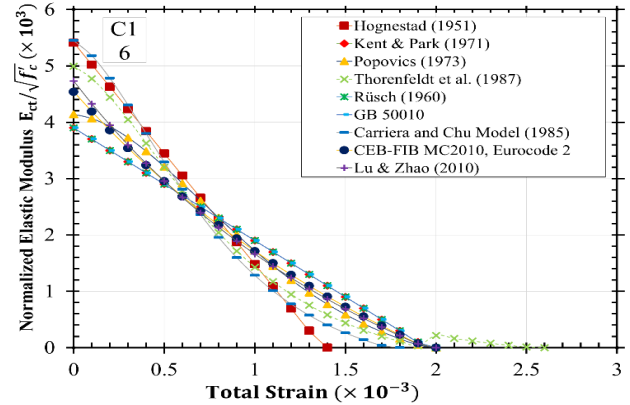


Fig. 3 Tangential Elastic Modulus  $E_{ct}$  behavior under increased loading up to peak stress

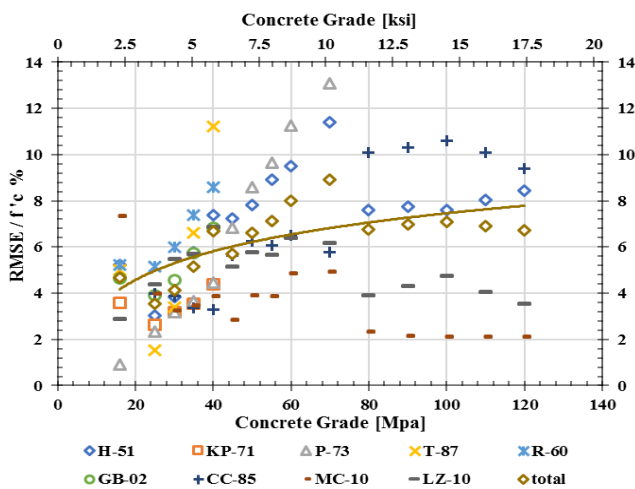


Fig. 2 RMSE values for different concrete constitutive models at various Grades

$fc'$ , adopted by ACI 318-14 (2014). Beyond the elasticity limit, models tend to result in high variability in estimating material response, with variability in the estimation of the point of peak strain. Upon reaching the compressive strength of the material, models prediction of post-peak behaviour is of high uncertainty. This uncertainty has resulted in the introduction of many refinements for post-peak behaviour.

It should be noted that results of Thorenfeldt model (1987) beyond concrete grade 70 MPa, have been omitted due to mathematical instability. Upon obtaining stress-strain diagrams for concrete grades of (16-120) MPa, the behaviour of each model has been investigated. Diverging results of different models have been omitted. The criteria for this selection being the comparison of resulting secant elastic modulus up to  $0.45 fc'$  resulting from all models, with the results of secant elastic modulus equations. It also based on the contribution of different models to the total mean square root of estimation for the material response. For concrete grades higher than 40 MPa, Kent & Park (1971) and Rüsçh (1960) models had been excluded, since these models have resulted in unreasonably high elastic modulus.

Also, Thorenfeldt *et al.* (1987) Model has been found to

Table 4 Root mean squared error (RMSE) values for different Models

Model	H-51	KP-71	P-73	T-87	R-60	GB-02	CC-85	MC-10	LZ-10	Mean Curve
RMSE, MPa	5.62	1.11	4.33	2.32	2.18	1.71	6.13	1.97	3.22	4.12

be unstable for grades higher than 70 MPa. So, it has been implemented only for lower grades. Popovics (1970) model has been excluded for grades higher than 70 MPa, due to estimating unreasonably high elastic modulus for higher concrete grades.

The calculated Root Mean Squared Error (RMSE) for the estimation of concrete response is given in Table 4. It is also presented the RMSE of various models from the mean value for the entire range of concrete grades. To bring these values of RMSE into perspective for each concrete grade, Fig. 2 shows the RMSE values as a percentage of concrete grades for the entire range of concrete grades. From this figure, the stability of models proposed by MC2010 (2010), Eurocode 2 (2004) and Lu and Zhao (2010) can be observed.

### 2.2 Elastic modulus estimation

The tangential elastic modulus of concrete in compression  $E_{ct}$ , defined as the slope of concrete stress-strain diagram at any stress. Based on the previously discussed concrete stress-strain models, the tangential elastic modulus can be found through differentiating each model with respect to strain, as follows

$$E_{ct} = \frac{d\sigma}{d\epsilon} \quad (25)$$

Upon differentiation of each model and substitution of incremental strain values, the behaviour of the tangential elastic modulus of concrete under incremental loading can be captured. Fig. 3 shows the behaviour of concrete tangential elastic modulus values normalized by the square root of the strength in compression.

It should be noted that negative values of the slope on the descending branch of the stress-strain diagram have been omitted. The reasons for that appear in two folds. on one hand, the peak strength of the concrete is not to be

Table 5 RMSE in estimating Tangential Elastic Modulus  $E_{ct}$ 

Model	H-51	KP-71	P-73	T-87	R-60	GB-02	CC-85	MC-10	LZ-10	Mean Curve
RMSE, GPa	3.44	1.65	3.28	1.26	1.65	1.65	3.47	2.00	3.82	2.98

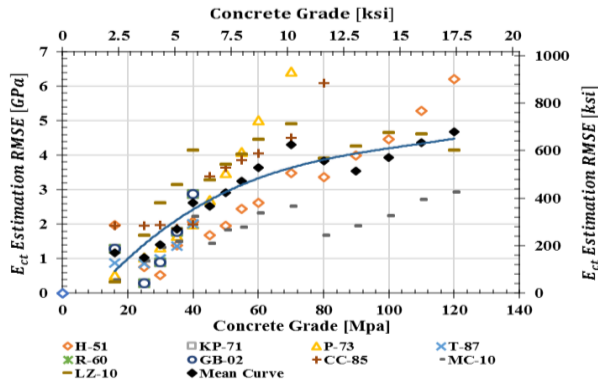


Fig. 4 Elastic modulus behavior under compression for Strength Grades 16-120 MPa

reached in design practice. On the other hand, the negativity of the stiffness can't be described. Moreover, post-peak behaviour has been found to depend on element size and testing procedure, rather than pure dependence on material strength and loading. For such reasons, in this paper, it is intended only to describe the ascending branch of concrete stress-strain diagram and the corresponding tangential elastic modulus. After combining these elastic modulus values based on aforementioned-models, the errors of estimate of the tangential elastic modulus are listed in Table 5 with respect to the mean of the data population.

The variation of RMSE values for each model at different concrete grades is presented in Fig. 4. Comparing RMSE values presented in this figure, to the secant elastic modulus values calculated using ACI 318-14 (2014) (Eq. (5.2.b)), results in a percentage representation of RMSE value that varying between 2.5% and 9% of  $E_c$ . this range is considered satisfactory considering variability of concrete samples used for the derivation of different models presented here with different mixtures and material sources. Also, such error values are comparable with errors revealed by other studies on concrete secant elastic modulus, (e.g., 10% in the case of Lu and Zhao (2010), 20% in the case of Pauw (1960) & ACI 318 equations (2-3). Through statistical analysis of normalized ( $E_{ct}/\sqrt{f'_c}$ ) versus concrete compressive stress level ( $\sigma/f'_c$ ), the following equation has been found to give the best estimation for tangential elastic modulus for concrete grades in the range 16-120 MPa.

$$E_{ct} = \varphi \cdot \sqrt{f'_c} \quad (26)$$

where Concrete Elasticity Index ( $\varphi$ ) is a function of the compressive stress level. This factor is included to account for the degradation of concrete stiffness in compression under increased loading.  $\varphi$  is equal to 4770 at initial loading; the initial tangent modulus  $E_{ci}$  and decrease to zero at peak stress; material strength (the zero is the theoretical limit, however, it was noted that due to regression errors, the value of the elasticity index is 220. Therefore, an error

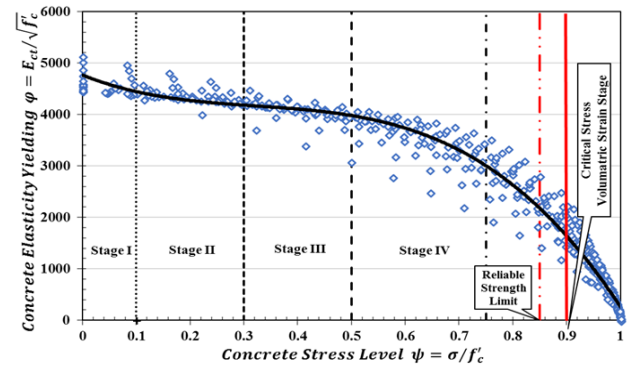


Fig. 5 Concrete Elasticity Index behavior and micro-cracking mechanism under increased loading

Table 6 Proposed Equation RMSE in estimating Tangential Elastic Modulus  $E_{ct}$ 

Grade	$E_{ct}$ RMSE, MPa	Grade	$E_{ct}$ RMSE, MPa
16	2212	60	934
25	1736	70	1477
30	1390	80	1380
35	1222	90	1734
40	1374	100	2112
45	937	110	2839
50	937	120	3827
55	818		

of 4.6% has been found. Which is satisfactory in comparison with practical errors in such modeling, (e.g., ACI 318-14, with up to 20% error in the elastic modulus estimation).

$$\varphi = (4.77 - 4.18 \cdot \psi + 10.73 \cdot \psi^2 - 11.10 \cdot \psi^3) \times 10^3 \quad (27)$$

where  $\psi$  is compressive stress level in concrete,  $\psi = (\sigma/f'_c)$ . Fig. 5 shows the behavior of concrete elasticity index  $\varphi$  versus concrete stress level  $\psi$ . Through data normalization of different models presented earlier for concrete grades between 16-120 MPa.

In the derivation of  $\varphi$  equation, as observed from Fig. 5, the multi-stages micro-cracking behavior of concrete under uniaxial compression has been acknowledged. At Stage I, from initial loading and up to  $\psi$  of 0.1, the initial tangent modulus value of vanish rapidly due to initial plastic strains (Mehta and Monteiro 2006). During stage II, between  $\psi$  value of 0.1 and up to 0.3 elastic modulus of concrete is almost stable and  $\varphi$  value decrease slightly from 4400 to 4200. At this stage the transition zone micro-cracks remain stable (Mehta and Monteiro 2006). At onset of stage III, that's  $\psi$  value of 0.3, the equation changes curvature so that, between 0.3 and up to 0.5 elastic modulus degradation increases with higher rate. This is in direct accordance with the increased number, dimensions of micro-cracks in the transition zone at this stress level (Mehta and Monteiro 2006). After exceeding  $\psi$  value of 0.5, that's stage IV in Fig. 5, cracks start propagating in the hardened cement matrix, in the vicinity of concrete transition zone. This results in a fast degradation in the concrete elastic modulus.

This appears clearly in the highly negative slope of  $\varphi$  in Fig. 5. Beyond the  $\psi$  value of 0.75,  $\varphi$  value maintains a steep declination till reaching zero stiffness at concrete peak stress (compressive strength). Investigating the error incorporated with proposed  $E_{ct}$  equation, the following table (Table 6) summarizes values of RMSE of estimation for  $E_{ct}$  of concrete grades in the range 16-120 MPa.

### 2.3 Reinforcement stiffness contribution

For reinforced concrete in unconfined compression, the effect of reinforcement on stiffness and tangent elastic modulus can be included, through the assumption of parallel stiffness. That's, through including the elastic modulus of reinforcement as

$$E_{RCt} = \rho' \cdot E_s + (1 - \rho') \cdot \varphi \cdot \sqrt{f'_c} \quad (28)$$

where  $\rho'$  is the reinforcement ratio, calculated as  $\rho' = A_s/A_{cc}$ , in which  $A_s$  and  $A_{cc}$  are the areas under compression of steel and concrete, respectively. Hence excluding portions of concrete and steel in tension for flexure members.

## 3. Nonlinear concrete constitutive relations

Following the introduction of  $E_{ct}$  and  $E_{RCt}$  equations, denoting the tangential elastic modulus, and equivalent reinforced concrete modulus. It is now possible, to use these stress dependent non-linear elastic moduli, in developing equations to describe the nonlinearity and lose of stiffness due to damage.

### 3.1 Concretes Nonlinear Hooke's law

Based on proposed stress dependent non-linear elastic moduli  $E_{ct}$  and  $E_{RCt}$ , in conjunction with stress-strain proportionality principal known as Hooke's law. Simply, by replacing the constant linear elastic modulus in hooks law with the proposed stress dependent moduli given by equations Eqs. (26) through (28) thus, the non-linear constitutive behavior of plain (Eq. (29)) and reinforced concrete (Eq. (30)), under compressive loading, are described as follows.

$$d\sigma = E_{ct} \cdot d\varepsilon = (\varphi \cdot \sqrt{f'_c}) \cdot d\varepsilon \quad (29)$$

$$d\sigma = E_{RCt} \cdot d\varepsilon = (\rho' \cdot E_s + (1 - \rho') \cdot \varphi \cdot \sqrt{f'_c}) \cdot d\varepsilon \quad (30)$$

Approximating the infinitesimal differential operators and applying numerical discretization to the integration between two stress levels results in the following. For plain concrete

$$\varepsilon_c = \sum_{i=0}^n \frac{(\sigma_i - \sigma_{i-1})}{E_{ct,i}} = \sum_{i=0}^n \frac{(\sigma_i - \sigma_{i-1})}{\varphi_i \cdot \sqrt{f'_c}} \quad (31)$$

For reinforced concrete

$$\varepsilon_{RC} = \sum_{i=0}^n \frac{(\sigma_i - \sigma_{i-1})}{(\rho' \cdot E_s + (1 - \rho') \cdot \varphi_i \cdot \sqrt{f'_c})} \quad (32)$$

Eqs. (30) and (31) can predict the non-linear stress-strain behaviour of plain and reinforced concrete,

respectively. These equations expand the applicability of Hooke's law beyond the assumed initial linearity, given by the secant modulus. Also, serves in simplifying the representation of concrete non-linearity in compression. Furthermore, equation Eq. (32) accounts for reinforcement presence in concrete subjected to compression especially for high reinforcement ratios and high-stress levels.

### 3.2 Concrete nonlinear strain energy density

Material non-linearity under increased loading can be described through the rate of internal energy accumulation. As stress level in concrete increases, strain energy density increases. However, the rate of such energy accumulation decreases as the material starts dissipating stored energy through cracks formation and propagation. That's, as the damage of the material increases, the capability of the material to gain more energy decreases. This rate approaches zero as the stress level approaches the peak stress. Internal energy density can be found through the integration of the area under material stress-strain diagram (Ugural and Fenster 2008).

$$U_0 = \int_0^\varepsilon \sigma \cdot \varepsilon \, d\varepsilon \quad (33)$$

where  $U_0$  denotes the strain energy density; which is the area under stress-strain diagram, having a unit of MPa (Ugural and Fenster 2008). However, Since  $E_{ct}$  and  $E_{RCt}$  equations are given in terms of stress level, and therefore stress, it is more desirable to find the energy strain density through the complementary energy density  $U_0^*$ ; the area above the stress-strain curve (Ugural and Fenster 2008).

$$U_0 = \sigma \cdot \varepsilon - U_0^* = \sigma \cdot \varepsilon - \int_0^\sigma \varepsilon \, d\sigma \approx \sigma \cdot \varepsilon - \sum_{i=0}^n \Delta\sigma \cdot \varepsilon_i \quad (34)$$

$$U_{0,n} = \sigma \cdot \sum_{i=0}^n \frac{(\sigma_i - \sigma_{i-1})}{\varphi_i \cdot \sqrt{f'_c}} - \sum_{i=0}^n (\sigma_i - \sigma_{i-1}) \cdot \sum_{i=0}^n \frac{(\sigma_i - \sigma_{i-1})}{\varphi_i \cdot \sqrt{f'_c}} \quad (35)$$

Which results in the following expressions for estimating the strain energy density  $U_0$  and the complementary energy density  $U_0^*$  for concrete, with strength-grades in the range 16-120 MPa.

$$\frac{U_{0,n}}{(\sqrt{f'_c})^3} = \psi_n \cdot \sum_{i=0}^n \left( \frac{\psi_i - \psi_{i-1}}{\varphi_i} \right) - \sum_{i=0}^n \left( (\psi_i - \psi_{i-1}) \cdot \sum_{i=0}^n \left( \frac{\psi_i - \psi_{i-1}}{\varphi_i} \right) \right) \quad (36)$$

$$\frac{U_{0,n}^*}{(\sqrt{f'_c})^3} = \sum_{i=0}^n \left( (\psi_i - \psi_{i-1}) \cdot \sum_{i=0}^n \left( \frac{\psi_i - \psi_{i-1}}{\varphi_i} \right) \right) \quad (37)$$

These equations can be applied easily through computer programming, yielding energy densities of concrete material as a function of only the stress level  $\psi$  and the concrete strength grade. It is worth noting, that the right-hand side of Eqs. (36) and (37) depends exclusively on loading extent, described by the stress level. This simplifies the introduction of material properties. Presented through the strength grade in the left-hand side. To assess concrete

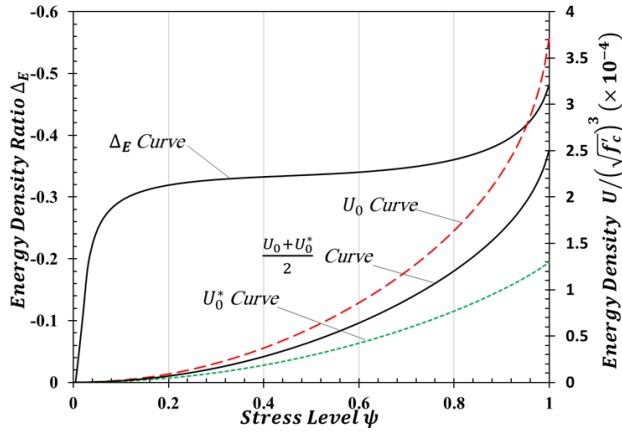


Fig. 6 Concrete energy densities variation with the stress level applied relative to the energy density ratio

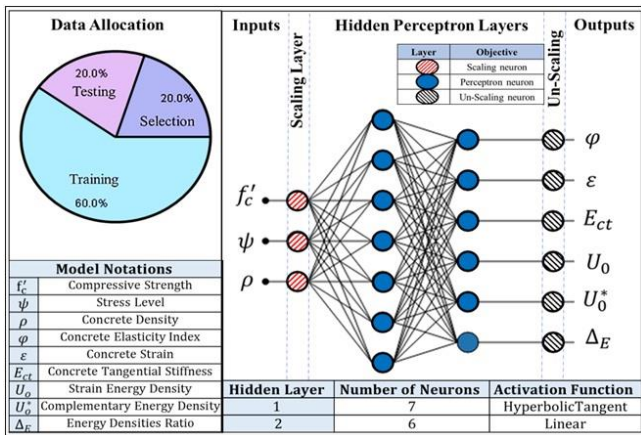


Fig. 7 Neural network training data allocation and model schematic architecture

stiffness yielding and degradation, it is possible to implement a unit less ratio of relative energy densities  $\Delta_E$ . Found as follows

$$\Delta_E = \frac{U_0^* - U_0}{U_0^* + U_0} \quad \{ \text{for } 0 < \psi \leq 1 \} \quad (38)$$

where  $U_0$  and  $U_0^*$  are as given by equation Eqs. (36) and (37), respectively. The use of  $\Delta_E$  as defined by equation Eq. (38) is to estimate in terms of energy density, the stiffness degradation relative to elastic material stiffness, which has an energy density of  $(U_0 + U_0^*)/2$ .  $\Delta_E$  value depends only on concrete stress level  $\psi$ , that at the same stress level, for any two concrete grades  $\Delta_E$  value would be the same. This ratio equal to zero for linear stages of stress strain behavior. However, once the concrete stiffness starts yielding and  $E_{ct}$  value start decreasing,  $\Delta_E$  value will start increasing. Fig. 6 shows the change of Energy Density ratio  $\Delta_E$  under increased loading from zero up to peak loading.

#### 4. Concrete nonlinearity through artificial neural network

Data as obtained from different models, aided with proposed formulations, have been introduced to the

Table 7 Neural network percentile error of estimate

Output Variable	Percentage Error %	
	Mean	Standard Deviation
$\varphi$	0.554	0.435
$\varepsilon$	2.413	3.289
$E_{ct}$	3.63	4.06
$U_0$	0.596	0.804
$U_0^*$	0.553	0.425
$\Delta_E$	1.705	2.192

computer to train a neural network (Ahmed and Muhannad (2018)) capable of predicting concrete behaviour and reduction of elasticity that would result due to an increased loading. Fig. 7 details the uses of all the instances in the dataset. The total number of instances is about 5000. divided into 60% training instances, 20% selection instances and 20% testing instances.

#### 4.1 Network architecture

A graphical representation of the resulted deep architecture is depicted in Fig. 7. It contains a scaling layer, a neural network and an un-scaling layer. The yellow circles represent scaling neurons, the blue circles perceptron neurons and the red circles un-scaling neurons. The number of inputs is 3, and the number of outputs is 6. The complexity, represented by the numbers of hidden neurons, is 7.

#### 4.2 Linear regression analysis

Testing the accuracy of the presented neural network model is performed through a linear regression analysis between the scaled neural network outputs and the corresponding targets for an independent testing subset. The resulting correlation coefficient  $R^2$  between the scaled outputs and the targets are listed in Fig. 8. Which show the estimation accuracy of the neural network in predicting Strain, Tangential Elastic Modulus, Concrete Elasticity Index, Energy Densities, and Energy densities ratio.

#### 4.3 Error data statistics

In-order-to assess the quality of the proposed neural network model, means and standard deviations of the errors between the neural network and the testing instances in the data set are summarized in Table 7.

### 5. Check the accuracy of the proposed models

In-order-to investigate the accuracy of the Proposed models, predicted concrete tangential elastic modulus  $E_{ct}$ , stress-strain constitutive behavior and energy densities  $U_0$  and  $U_0^*$ , using proposed equations and neural network has been compared to many experimental results published elsewhere. Using proposed neural network, the stress-strain diagrams for concrete grades in the range 10-120 MPa up to

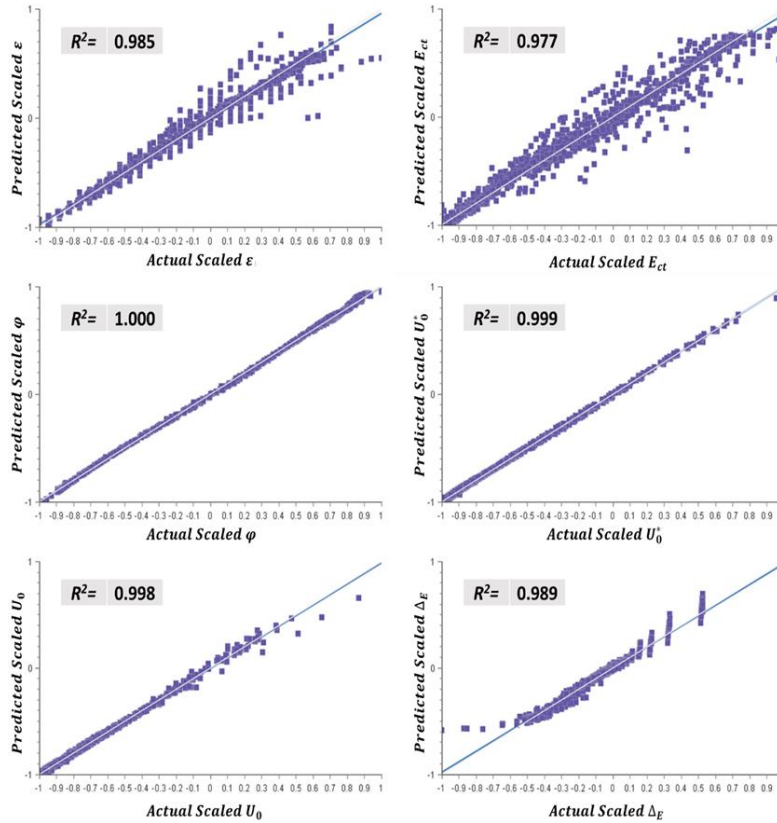


Fig. 8 Neural network prediction accuracy of various outputs

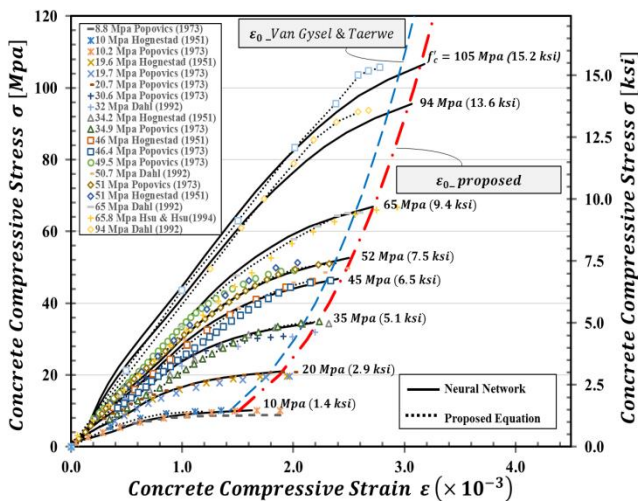


Fig. 9 Validation of proposed stress-strain model and neural network with experimental results for various concrete grades

peak stress are depicted in Fig. 9. This figure shows good agreement between experimental results and neural network-obtained stress-strain diagrams. The peak stress as predicted by proposed neural network correspond to a strain given by the equation

$$\epsilon_0 = 740 \times 10^{-6} \cdot f_c'^{0.31} \quad (39)$$

This equation is a modification of the following equation proposed by Van Gysel and Taerwe (1996). Such modification serves to increase the accuracy for concrete

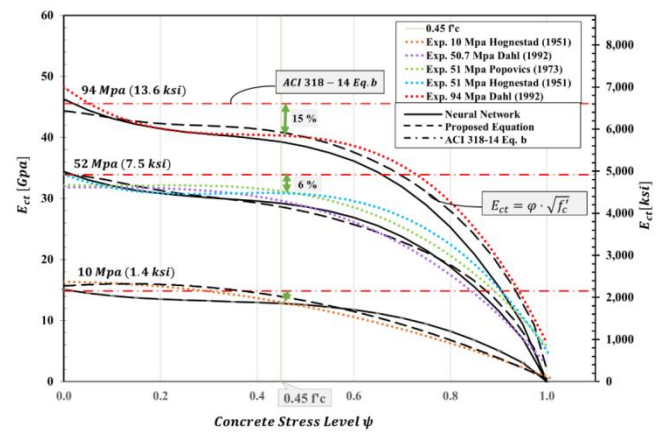


Fig. 10 Predicted concrete elastic modulus validation with experimental results

grades up to 80 MPa. However, for higher concrete grades both equations predicts higher strains and higher deformation at peak stress. This higher prediction serves in providing a margin of conservativeness regarding serviceability. Fig. 10 shows the accurate prediction of the elastic modulus  $E_{ct}$  using proposed equation and network. In this figure, the constant elastic modulus equation proposed by ACI 318 (2014) is depicted. It is observed that the ACI 318 (2014) equation yields satisfactory results for stress levels up to  $0.45 f_c'$  only for concrete grades less than 52 MPa, overestimating the elastic modulus for high strength concrete. This agrees with findings by other researchers (Nilson *et al.* 2010, Carraquillo *et al.* 1981).

```

% The mathematical expression represented by the neural network is written below. It takes the inputs Concrete Grade, stress/f c and
% reinforcement ratio (rho) to produce the outputs Total Strain, Ect, Phi, U*, U0 and delta. For function regression problems, the information
% is propagated in a feed-forward fashion through the scaling layer, the perceptron layers and the un-scaling layer.
% Scaling Layer Receives Inputs
scaled_Concrete_Grade=(Concrete_Grade-61.5944)/31.2921;
scaled_stress_f_c=(stress_f_c-0.645539)/0.317569;
scaled_rho=(rho-0.00276308)/0.00355394;
% First Hidden Perceptron Layer Receives Scaled Inputs;
y11=tanh(0.223889+0.217256*scaled_Concrete_Grade-0.153047*scaled_stress_f_c-0.00355984*scaled_rho);
y12=tanh(-1.08079+0.124451*scaled_Concrete_Grade-0.684099*scaled_stress_f_c-0.0112626*scaled_rho);
y13=tanh(3.43971+0.0075667*scaled_Concrete_Grade-2.62327*scaled_stress_f_c-0.010781*scaled_rho);
y14=tanh(-0.776147+0.0520378*scaled_Concrete_Grade+1.19881*scaled_stress_f_c-0.00263114*scaled_rho);
y15=tanh(-3.81515-0.173961*scaled_Concrete_Grade-2.27273*scaled_stress_f_c+0.00102226*scaled_rho);
y16=tanh(1.40959-0.244396*scaled_Concrete_Grade-0.764311*scaled_stress_f_c-0.00405507*scaled_rho);
y17=tanh(2.12837+0.465488*scaled_Concrete_Grade-0.554236*scaled_stress_f_c-0.137561*scaled_rho);
% Second Hidden Perceptron Layer Receives The First Layer Outputs To Compute The Scaled Responses;
scaled_Total_Strain=(-1.42183+0.93381*(y11)-0.897862*(y12)-0.634284*(y13)+0.476152*(y14)+0.100205*(y15)...
+0.0960811*(y16)+1.20427*(y17));
scaled_Ect=(-1.64129+2.36922*(y11)-0.518283*(y12)+0.379532*(y13)+0.195001*(y14)+0.100598*(y15)+1.8513*(y16)-1.08777*(y17));
scaled_Phi=(-0.690017+0.185434*(y11)-0.148541*(y12)+0.770819*(y13)-0.869979*(y14)+0.176942*(y15)-0.0434904*(y16)...
-0.0934151*(y17));
scaled_U*=(0.789478+0.413806*(y11)-0.380497*(y12)+0.319245*(y13)-0.314743*(y14)+0.114167*(y15)-2.59785*(y16)+0.00827042*(y17));
scaled_U0=(0.746213+0.137679*(y11)-0.184493*(y12)+0.0242184*(y13)-0.340061*(y14)+0.0588924*(y15)-2.38007*(y16)+0.209227*(y17));
scaled_delta=(0.116646-0.3925*(y11)+0.21269*(y12)+0.750063*(y13)-0.230452*(y14)+0.534374*(y15)-0.473538*(y16)+0.192451*(y17));
% The Un-Scaling Layer Performs The Following Computations To Compute The Results Vector;
(Total_Strain,Ect,Phi,U*,U0,delta)=(0.5*(scaled_Total_Strain+1.0)*(0.0034-0)+0,0,5*(scaled_Ect+1.0)*(53689.2-0)...
+0,0,5*(scaled_Phi+1.0)*(4770+37.5637)-37.5637,0,5*(scaled_U*+1.0)*(0.173895-0)...
+0,0,5*(scaled_U0+1.0)*(0.471133-0)+0,0,5*(scaled_delta+1.0)*(0+0.613975);

```

Fig. 11 Neural network sub-routine code for the assessment of concrete elasticity

## 6. Summary

In this section, non-linear material models have been proposed, capturing the behavior of plain and reinforced concrete under uniaxial compression. Accounting for the micro scale cracks formation and propagation. Prediction of Tangential elastic modulus for plain and reinforced concrete has been facilitated through the equation

$$E_{Rct} = \rho' \cdot E_s + (1 - \rho') \cdot \varphi \cdot \sqrt{f'_c} \quad (40)$$

Concrete constitutive stress-strain behavior has been facilitated through Hooke's law by replacing the constant secant elastic modulus with the stress-dependent tangential elastic modulus. Consequently, the ascending branch of concrete stress-strain diagram can be predicted for concrete grades of 10-120 MPa.

$$\varepsilon_{RC} = \sum_{i=0}^n \frac{(\sigma_i - \sigma_{i-1})}{\left( \rho' \cdot E_s + (1 - \rho') \cdot \varphi \cdot \sqrt{f'_c} \right)} \quad (41)$$

Energy densities of concrete has been derived as follows

$$\frac{U_{0,n}}{(\sqrt{f'_c})^3} = \psi_n \cdot \sum_{i=0}^n \left( \frac{\psi_i - \psi_{i-1}}{\varphi_i} \right) - \sum_{i=0}^n \left( (\psi_i - \psi_{i-1}) \cdot \sum_{i=0}^n \left( \frac{\psi_i - \psi_{i-1}}{\varphi_i} \right) \right) \quad (42)$$

$$\frac{U_{0,n}^*}{(\sqrt{f'_c})^3} = \sum_{i=0}^n \left( (\psi_i - \psi_{i-1}) \cdot \sum_{i=0}^n \left( \frac{\psi_i - \psi_{i-1}}{\varphi_i} \right) \right) \quad (43)$$

A neural network capable of predicting the behavior of concrete in terms of stiffness and strain at any stress level for concrete grades ranging from 16 to 120 MPa. The code for implementing the neural network as a sub-routine into computer programming is provided in Fig. 13. It takes the inputs Concrete Grade, stress/ $f_c$  and reinforcement ratio

(rho) to produce the outputs Total Strain,  $E_{ct}$ ,  $\Phi$ ,  $U^*$ ,  $U_0$  and delta. For function regression problems, the information is propagated in a feed-forward fashion through the scaling layer, the perceptron layers and the un-scaling layer.

## 7. Conclusions

Based on this study, the following conclusions can be drawn:

1. The constitutive models proposed by many researchers have been used to generate novel stiffness parameters and constitutive curves for concrete. The consideration of many models is to account for various shapes of concrete stress-strain diagrams that result due to the randomness of mixtures, compositions and material sources.
2. The constitutive models proposed by many researchers have been used to generate novel stiffness parameters and constitutive curves for concrete. The consideration of many models is to account for various shapes of concrete stress-strain diagrams that result due to the randomness of mixtures, compositions and material sources.
3. Concrete stress-strain diagrams for concrete grades ranging from 16 to 120 MPa have been considered. Covering very weak mixes of non-structural concrete, to ultra-high strength concrete. Each model behavior has been investigated for the entire range of concrete grades to examine stability and results-reliability of different models in comparison to the more refined ones
4. The accuracy of the proposed tangential elasticity is compared with the ACI 318-14 (2014) secant elastic modulus. It has been found that, the resulting percentile RMSE value, varying between 2.5% and 9% of  $E_c$ , has increased the accuracy of elasticity estimate in comparison with errors revealed by other researcher's

equations.

5. The concept of Concrete Elasticity Index ( $\varphi$ ) has been proposed and this factor has been introduced to account for the degradation of concrete stiffness in compression under increased loading ( $\psi$ ).

6. In acknowledging the reinforcement contribution to concrete elasticity, the concept of parallel stiffness has been applied which is resulting a new proposed equation for estimating the reinforced concrete elastic modulus.

7. In the derivation of ( $\varphi$ ) equation, the multi-stages micro-cracking behaviour of concrete under uniaxial compression has been acknowledged. Thus, from initial loading and up to a stress level ( $\psi$ ) of 0.1, the initial elasticity index value declines rapidly due to the influence of the initial plastic strains in degrading the initial tangent modulus. Furthermore, between ( $\psi$ ) value of 0.1 and up to 0.3, the elasticity index stabilizes with a marginal decrease from 4400 to 4200. At this stage, the micro-cracks in the aggregate-cement-matrix transition zone remain stable. At the onset of a 0.3 stress level, the elasticity index changes curvature, so that, between 0.3 and up to 0.5 elastic modulus degradation increases with a higher rate. In a manifestation of the increased number, dimensions of the transition-zone micro-cracks. After exceeding a ( $\psi$ ) value of 0.5, cracks start propagating in the hardened cement matrix, in the vicinity of the concrete transition zone. This results in a fast degradation in the concrete elasticity index. This appears clearly, in the highly-negative declination of the slope of ( $\varphi$ ). Beyond the ( $\psi$ ) value of 0.75, ( $\varphi$ ) value maintains a steep declination till the full diminish at the concrete peak stress (the compressive strength).

8. The proposed Young's stress-strain can replace the constant linear elastic modulus by using approximations of the infinitesimal differential operators, through applying numerical discretization of the integral function, describing the non-linear constitutive behaviour of plain and reinforced concrete under compressive loading. These proposed equations expand the applicability of Hooke's law beyond the assumed initial linearity, given by the secant modulus. Also, serves in simplifying the representation of concrete non-linearity in compression.

9. The stiffness deterioration analysis of concrete material (strength-grades in the range from 10 to 140 MPa) have been proposed for estimating the strain energy density ( $U_0$ ) and the complementary energy density ( $U_0^*$ ) for concrete. This proposed equations depends exclusively on the loading extent which described by the stress level. Therefore, this simplifies the introduction of material properties through the strength grade on the left-hand side.

10. The material non-linearity under increased loading can be described through the rate of internal energy accumulation. As stress level in concrete increases, strain energy density increases. However, the rate of such energy accumulation decreases as the material starts dissipating stored energy through cracks formation and propagation. That's, as the damage of the material increases, the capability of the material to gain more

energy decreases. This rate approaches zero as the stress level approaches the peak stress.

11. A sub-routine artificial neural network model has been developed, to facilitate the computerization of concrete response recognition and prediction. Its outputs have been validated with experimental instances and revealed a remarkable accuracy.

## References

- ACI committee 318 (1963), Building Code Requirements for Structural Concrete 318-63, MI
- ACI Committee 318 (2014), Building Code Requirements for Reinforced Concrete, (ACI 318-14) and Commentary (318R-14), American Concrete Institute, Farmington Hills, M.I., 443.
- ACI Committee 363 (1997), State-of-the-Art Report on High-Strength Concrete (ACI 363R-92).
- Ashteyat, A.M. and Ismeik, M. (2018), "Predicting residual compressive strength of self-compacted concrete under various temperatures and relative humidity conditions by Artificial Neural Networks", *Comput. Concrete*, **21**(1), 47-54.
- BS EN 1992-1-1 (2004), Eurocode 2: Design of concrete structures - Part 1-1 : General Rules and Rules for Buildings,
- Carrasquillo, R.L., Nilson, A.H. and Slate, F.O. (1981), "Properties of high strength concrete subject to short-term load", *J. Proc.*, **78**(3), 171-178.
- Carreira, D.J. and Chu, K.H. (1985), "Stress-strain relationship for plain concrete in compression", *J. Am. Concrete Inst.*, **82**(6), 797-804.
- Dias, M.M., Tamayo, J.L., Morsch, I.B. and Awruch, A.M. (2015), "Time dependent finite element analysis of steel-concrete composite beams considering partial interaction", *Comput. Concrete*, **15**(4), 687-707.
- GB 50010-2002 (2002), Code for Design of Concrete Structures, 211.
- Hognestad, E. (1951), "Study of combined bending and axial load in reinforced concrete members", University of Illinois at Urbana Champaign, College of Engineering, Engineering Experiment Station.
- International Federation for Structural Concrete (2013), fib Model Code for Concrete Structures 2010 MC2010, fib Model Code Concrete Structure 2010.
- Kent, D.C. and Park, R. (1971), "Flexural members with confined concrete", *J. Struct. Div.*, **97**, 1969-1990
- Liang, J.F., Yang, Z.P., Yi, P.H. and Wang, J.B. (2015), "Mechanical properties of recycled fine glass aggregate concrete under uniaxial loading", *Comput. Concrete*, **16**(2), 275-285.
- Liang, J.F., Yang, Z.P., Yi, P.H. and Wang, J.B. (2017), "Stress-strain relationship for recycled aggregate concrete after exposure to elevated temperatures", *Comput. Concrete*, **19**(6), 609-615.
- Lu, Z.H. and Zhao, Y.G. (2010), "Empirical stress-strain model for unconfined high-strength concrete under uniaxial compression", *J. Mater. Civil Eng.*, **22**(11), 1181-1186.
- Maia, L. and Aslani, F. (2016), "Modulus of elasticity of concretes produced with basaltic aggregate", *Comput. Concrete*, **17**(1), 129-140.
- Martinez, S., Nilson, A.H. and Slate, F. (1984), "Spirally reinforced high-strength concrete columns", *ACI J. Proc.*, doi: 10.14359/10693.
- Mehta, P.K. and Monteiro, P.J.M. (2006), "Concrete: microstructure, properties, and materials", *Concrete*, Doi: 10.1036/0071462899.
- Nilson, A.H., Darwin, D. and Dolan, C.W. (2010), "Design of

- concrete structures”,
- Noguchi, T., Tomosawa, F., Nemati, K.M., Chiaia, B.M. and Fantilli, A.P. (2009), “A practical equation for elastic modulus of concrete”, *ACI Struct. J.*, **106**, 690-696
- Pandey, A.K. (2013), “Flexural ductility of RC beam sections at high strain rates”, *Comput. Concrete*, **12**(4), 537-552.
- Pauw, A. (1960), *Static Modulus of Elasticity of Concrete as Affected by Density*, University of Missouri.
- Popovics, S. (1970), “A review of stress-strain relationships for concrete”, *J. Proc.*, **67**(3), 243-248.
- Rusch, H. (1960), “Researches toward a general flexural theory for structural concrete”, *J. Am. Concrete Inst.*, **57**, 1-28
- Sargin, M. and Handa, V. (1969), “A general formulation for the stress-strain properties of concrete”, SM Report Solid Mechanics Division, University of Waterloo, Canada.
- Shahbeyk, S., Moghaddam, M.Z. and Safarnejad, M. (2017), “A physically consistent stress-strain model for actively confined concrete”, *Comput. Concrete*, **20**, 85-97.
- Thorenfeldt, E. Tomaszewicz, A. and Jensen, J.J. (1987), “Mechanical properties of high-strength concrete and application in design”, *Proceedings of the Symposium Utilization of High-Strength Concrete*, Tapir, Trondheim.
- Ugural, A.C. and Fenster, S.K. (2008), *Advanced Strength and Applied eElasticity*, 4th Edition, Meas Methane Prod from Ruminants.
- Van Gysel, A. and Taerwe, L. (1996), “Analytical formulation of the complete stress-strain curve for high strength concrete”, *Mater. Struct.*, **29**, 529-533.
- Yadollahia, M.M. and Benli, A. (2017), “Stress-strain behavior of geopolymer under uniaxial compression”, *Comput. Concrete*, **20**(4), 381-389.